Am J Transl Res 2019;11(4):2013-2027
www.ajtr.org /ISSN:1943-8141/AJTR0082367

Original Article

Pleiotrophin regulates functional heterogeneity of microglia cells in EAE animal models of multiple sclerosis by activating CCr-7/CD206 molecules and functional cytokines

Jiayin Miao[1*], Feng Wang[3,4*], Ru Wang[1], Jianqi Zeng[1], Cina Zheng[2], Guohong Zhuang[5]

[1]Department of Neurology, [2]Magnetic Resonance Center, Zhongshan Hospital, Xiamen University, 201 Hubinnan Road, Xiamen 361004, China; [3]College of Computer Engineering, Jimei University, Xiamen 361021, China; [4]Department of Electronic Science, Fujian Provincial Key Laboratory of Plasma and Magnetic Resonance, Xiamen University, Xiamen 361005, China; [5]Organ Transplantation Institute, Anti-Cancer Research Center, Medical College, Xiamen University, Xiamen 361000, China. [*]Equal contributors.

Received July 10, 2018; Accepted January 20, 2019; Epub April 15, 2019; Published April 30, 2019

Abstract: Multiple sclerosis (MS) is a neurodegenerative and immune-mediated disorder that characterizes by demyelination and neuro-inflammation. This study aimed to investigate the effects of pleiotrophin (PTN) on treatment of early injuries of white matter of MS patients. Experimental autoimmune encephalomyelitis (EAE) animal models were established by injecting 200 μg myelinoligodendrocyte glyeoprotein 33-35 (MOG35-55) and were divided into PTN+MOG group and PBS+MOG group. Meanwhile, normal mice group was assigned as control group (NC group). Immunofluorescence double label was used to examined co-expression of molecules. LV5-PTN and LV3-siPTN were established and transfected into microglia cells. All brain imaging data was acquired with MRI scanner. Quantitative real-time RT-PCR (qRT-PCR) and western blot were used to evaluate mRNA and protein expression, respectively. Lesion sites mainly appeared in NAWM of bilateral occipital lobes in EAE models. PTN treatment significantly enhanced CCr7 and reduced CD206 expression compared to PBS+MOG group ($P<0.05$). PTN participated in mitogen-activated protein kinase (MAPK) signaling pathway in EAE models. PTN treatment significantly regulated levels of functional cytokines in both M1 and M2 type microglia cells compared to PBS+MOG group ($P<0.05$). LV5-PTN and LV3-siPTN transfection modulated levels of PTN and MAPK molecule in microglia cells undergoing treatment of M1 or M2 inducer. PTN strengthened M1/M2 transformation by regulating functional cytokines. In conclusion, PTN regulated functional heterogeneity of microglia cells in EAE animal models of MS by activating CCr-7/CD206 molecules and functional cytokines. PTN could be considered as a promising candidate molecule for treating early injuries of white matter of patients with MS.

Keywords: Multiple sclerosis, functional heterogeneity, pleiotrophin, experimental autoimmune encephalomyelitis

Introduction

Multiple sclerosis (MS) is a progressive, neurodegenerative and immune-mediated disorder that characterizes by the demyelination and neuro-inflammation in central nervous system (CNS) [1, 2]. The epidemiological investigations reported that the incidence of MS has been significantly increased in the past years [3, 4]. However, the associated mechanisms have not been clarified and the treatments were still with lower-efficacy in clinical [5, 6]. Nowadays, the most applied therapeutic method for MS is the immuno-modulatory treatment, which mainly plays the therapeutic roles by reducing or inhibiting infiltration immune-cells into the central nervous system [7]. The previous study [8] reported that glucocorticoids could also regulate the growth of inflammatory cells and modulate the migration of inflammatory cells to the central nervous system. Meanwhile, the glucocorticoids could reduce the severity of relapse and accelerate the recovery of diseases. Donia et al [9] found that dexamethasone significantly reduced or relieved the clinical symptoms and disorder duration of the experimental autoim-

mune encephalomyelitis (EAE), which is an extensively used animal model for MS.

In clinical, eliminating progression or relapsing of neurological disability of MS is the difficulty of the clinical therapy. The activated microglia cells migrate to pre-active lesions-normal appearing white matter (NAWM) of MS lesion at earliest stage [10, 11]. Therefore, the microglia activation is considered to be an initial pathogenetic event for MS [12]. However, the nature that activates the resident microglia cells and triggers the related inflammatory reactions in NAWM remain to be elucidated.

Classically activated (M1) and alternatively activated (M2) microglia are two extremes of activation states. Activated M1cells produce large amounts of pro-inflammatory cytokines, all of which contribute to the development and pathogenesis of EAE in early phase M1 cells [13, 14]. M2 microglia highly expresses the anti-inflammatory molecules, all of which play the roles of anti-inflammation and tissue repair [15]. The NAWM in the pathogenesis processes of MS is also in a balance between neuro-protection and inflammation [16]. Therefore, we speculated that striking this balance may discover a feasible selection for treatment of MS.

Pleiotrophin (PTN), as a kind of secreted growth factor, plays the protective effects and post-developmental neurotrophic effects on the central nervous system [17]. PTN could promote the remyelination and expression of which increases in microglia post the ischemia/reperfusion [18, 19]. Our previous study proved that PTN plays a key role in the regulation of microglia by stimulating secretion of neuro-protective factors and promoting the cell proliferation [20].

Therefore, the present study used DTI and histopathology correlation to test whether PTN could modulate two extremes of microglial activation states proportion in NAWM of EAE. Meanwhile, the molecular signals contributing to this function were also examined *in vitro* levels.

Materials and methods

Animals

Forty 10-week-old male C57BL/6L mice, weighting 18±2 g, were purchased from Animal Center of the Third Military Medical University, Chongqing, China. All mice were kept under pathogen-free conditions. The rats were maintained in condition of 12 h light/12 h dark cycle at temperature of 25°C ± 2°C. The mice freely accessed to standard commercial diet (CLEA Japan Inc., Shizuoka, Japan) and water.

This study was performed according to the guidance of Care and Use of Laboratory Animals of National Institute of Health (NIH). The animal experiments were approved by the Ethics Committee of Zhongshan Hospital, Xiamen University (Xiamen, Fujian Province, China).

Establishment of EAE animal model

In order to induce the EAE, the following processes were conducted in this study (**Figure 1A**). In brief, the mice were immunized with a injection containing 200 μg myelinoligodendrocyte glyeoprotein 33-35 (MOG35-55) (GL Biotech. Ltd., Shanghai, China) in 200 μl phosphate-buffered saline (PBS) that emulsified by the complete Freund's adjuvant (CFA, Sigma-Aldrich, St. Louis, Missouri, USA) (1:1 ratio). On the day 0, each mouse received MOG-CFA emulsion by subcutaneously injecting into two sites of the upper flanks. The mice were subsequently intraperitoneally (i.p.) injected with 200 μl of pertussis toxin (200 ng, Sigma-Aldrich, St. Louis, Missouri, USA), which was repeated at 2 days post-immunization (p.i.). For the control mice, which were only immunized with CFA only in the experiments.

Grouping of EAE animal models

All of the EAE models were divided into two groups, including PBS+MOG group (20 mice) and PTN+MOG group (20 mice). At day 7 post the immunization (symptoms onset), the drug treatment was initiated by intraperitoneally injecting with either 1 μg/μl of PTN (ApexBio Tech., Texas, USA) in saline (PTN+MOG group) or PBS alone (PBS+MOG group). Meanwhile, the mice without any treatment were assigned as the normal control group (NC group) for the following tests.

Immunofluorescence double label assay

The tissues were fixed and permeabilized with 4% paraformaldehyde (Sangon Biotech. Co. Ltd., Shanghai, China) and 0.5% Triton X-100 (Sangon Biotech. Co. Ltd.). Then, the tissues

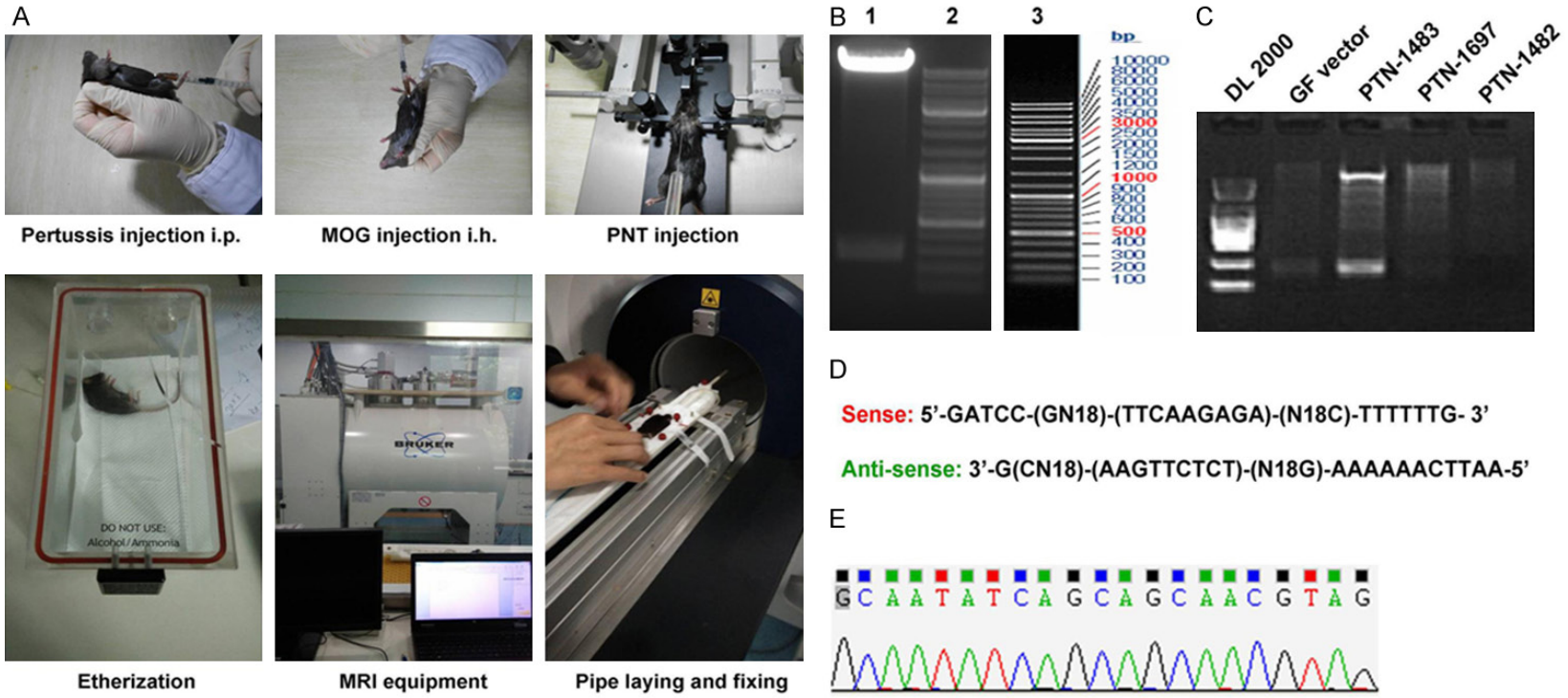

Figure 1. Animal model establishment and observation for LV5-PTN and LV3-siPTN lentivirus packing and transfection into microglia cells. A. Graphs for the processes of EAE animal model establishment. B. Plasmid construction of LV5-PTN and LV3-siPTN. C. Identification of PTN expression. D. Oligonucleotide sequence for small interfere RNAs. E. Identification for sequence of oligonucleotide sequence.

were treated with ethanol for 10 min at different concentrations and incubated with xylene for 10 min at different concentrations, and then embedded into the paraffin according to the previously published study [21]. For double staining of target molecules (including Mac-1, PTN, CCr-7, CD206, p-ERK1/2, p-JNK, p-P38), the tissues were firstly incubated with rabbit anti-mouse PTN polyclonal antibody (1:2000; Abcam Biotech, Cambridge, Massachusetts, USA), rabbit anti-mouse CCr-7 polyclonal antibody (1:2000, Abcam Biotech.), rabbit anti-mouse CD206 polyclonal antibody (1:2000, Abcam Biotech.), rabbit anti-mouse p-ERK1/2 polyclonal antibody (1:2000, Abcam Biotech.), rabbit anti-pJNK polyclonal antibody, rabbit anti-mouse p-p39 polyclonal antibody and stained with goat anti-rabbit antibody conjugated with FITC (Abcam Biotech.). Then, the tissues were denatured by using 2 M HCl for 10 min at 37°C, and incubated with rabbit anti-mouse Mac-1 polyclonal antibody (Abcam Biotech, Cambridge, Massachusetts, USA). The tissues were then stained with goat anti-mouse antibody conjugated with Alexa Fluor 647 (Abcam Biotech.). The tissues were mounted in an anti-fade containing medium with 0.25 μg/ml of 4',6-diamidino-2-phenylindole (DAPI, Biyotime Biotech. Shanghai, China) as a DNA counter stain. Then, fluorescence images were captured with a Laser scanning confocal microscope (Leica, Frankfurt, Germany) fitted with appropriate filters for FITC and Texas Red.

Plasmid construction, lentivirus packaging and transfection into microglia cells

In this study, the pG-LV5 lentiviral vector (LV5) and pG-LV3 lentiviral vector (LV3) (GenePhama Co. Ltd, Shanghai, China) were employed to construct LV5-PTN and LV3-siPTN, respectively. Oligonucleotides for constructing PTN genes (for pG-LV5 plasmid) and interfere PTN genes (for pG-LV-3 plasmid) were designed and synthesized by GenePhama Co. Ltd. (Shanghai, China). We screened 3 oligonucleotides and selected one oligonucleotide as the targeting PTN gene sequence (PTN-1483 gene) for establishing the LV5-PTN plasmid, which exhibited higher-density of gene bands (**Figure 1B**, **1C**). Oligonucleotide sequence for small interfere RNA was listed in **Figure 1D**, and sequence of which was identified to be correct (**Figure 1E**). The DNA double-chains were artificially synthesized by employing GenePhama Co. Ltd. (Shanghai, China). Finally, the synthesized double-chain sequences of both PTN genes and siPTN genes were sub-cloned into pG-LV5 and pG-LV3 plasmid to construct the LV5-PTN and LV3-siPTN plasmid, respectively.

LV5-PTN and LV3-siPTN plasmid and packing plasmids (PG-p1-VSVG, PG-P2-REV, PG-P3-RRE) were transfected with RNAi-mate (GenePhama Co., Ltd, Shanghai, China), according to manufacturer's instruction. The viral packaging processes were conducted due to the description of the previous study reported [22]. Then, the microglia cells were infected with LV5-PTN and LV3-siPTN, supplementing with 5 μg/ml polybrene (GenePhama Co. Ltd, Shanghai, China) for the following experiments.

MRI acquisition

All brain imaging data were acquired by using BIOSPEC 70/20 USR MRI scanner (BioSpec, Bruker, Ettlingen, Germany). A standardized imaging protocol was used and a rigorous quality control was also conducted to confirm the accuracy of data. A sagittal T1-weighted 3D spoiled radient-recalled echo (SPGR) sequence (TR/TE=22/8 ms, 1 signal average, 250 mm FOV, 1.5 mm slice thickness, 30° flip angle) was acquired for region of interest (ROI) definition, along with an axial proton-density/T2 weighted dual-echo sequence (TR=3500 ms, TE=15 ms and 63 ms, 1 signal average, 90° axial slices, 250 mm FOV, 2 mm thick contiguous slices, 256×256 matrix, 90° flip angle). For diffusion tensor calculation, a single shot spin-echo sequence with an EPI readout, TR=8300 ms, TE=79 ms, 32 contiguous axial slices, 5 mm thick, and 128×128 matrix was used to acquire one on-diffusion-weighted (b=0) and 25 diffusion-weighted (b=1000 s/mm^2) images with different diffusion-encoding directions. The acquisition of 25 diffusion directions used here afforded more robust tensor estimation as compared to former studies that relied on 8 directions [23, 24].

Quantitative real-time RT-PCR (qRT-PCR)

The RNAs of microglia cells were extracted with the TRIzol regents (Beyotime Biotech. Shanghai, China). The Reverse Transcription regents (Western Biotech., Chongqing, China) was use to synthesize complementary DNAs

Table 1. Primer sequences for the qRT-PCR

Genes		Sequences	Length (bp)
TNF-α	Forwards	CCCTCCAGAAAAGACACCATG	183
	Reverse	CACCCCGAAGTTCAGTAGACAG	
IL-18	Forwards	AATGGAGACCTGGAATCAGACA	160
	Reverse	TCAGTCTGGTCTGGGGTTCA	
IL-10	Forwards	GGACAACATACTGCTAACCGACTC	110
	Reverse	CCTGGGGCATCACTTCTACC	
TGF-β	Forwards	GGCGGTGCTCGCTTTGTA	136
	Reverse	GATGGCGTTGTTGCGGTC	
β-actin	Forwards	GAGACCTTCAACACCCCAGC	236
	Reverse	ATGTCACGCACGATTTCCC	

(cDNAs) according to the manufacturer's instruction. The qRT-PCR assay was conducted with the Sybgreen I kit (Western Biotech. Chongqing, China) as the fluorescent dye, and conducted on a Real-time PCR system (Eppendorf, Hamburg, Germany). Amplification of qRT-PCR was conducted as the following conditions: 94°C for 4 min, 94°C for 20 s, 60°C for 30 s, 72°C for 30 s, for 35 cycles. The qRT-PCR primers for tumor necrosis factor α (TNF-α), interleukin 10 (IL-10), interleukin 18 (IL-18), transforming growth factor β (TGF-β) and β-actin were listed in **Table 1**. The amplified products were loaded onto 1.5% agarose gels, and the images were captured and analyzed with UVP image scanning system (Mode: GDS8000, Sacramento, CA, USA). The relative mRNA levels of targeting genes were normalized to the β-actin gene with the comparative threshold cycle ($2^{-\Delta\Delta CT}$) method.

Western blot assay

The proteins were extracted from the microg lia cells by using radioimmunoprecipitation assay (RIPA) lysis buffer (Beyotime Biotech., Shanghai, China) and separated with the 15% sodium dodecyl sulfate polyacrylamide gel electrophoresis (SDS-PAGE, Amersham Biosciences, Little Chalfont, Buckinghamshire, England). The extracted proteins were electrotransferred onto polyvinylidene fluoride (PVDF, Dupont, USA). PVDF membranes were blocked with 5% bovine serum albumin (BAS) in PBS and incubated with rabbit anti-mouse PTN polyclonal antibody (1:3000; Abcam Biotech., Cambridge, Massachusetts, USA), rabbit anti-mouse extracellular regulated kinase 1/2 (ERK1/2) polyclonal antibody (1:2000; Abcam Biotech.), rabbit anti-mouse phosphorylated ERK1/2 (p-ERK1/2) polyclonal antibody (1:2000; Abcam Biotech.), rabbit anti-mouse extracellular regulated kinase 5 (ERK5) polyclonal antibody (1:3000, Sigma-Aldrich, St. Louis, Missouri, USA), rabbit anti-mouse phosphorylated ERK5 (p-ERK5) monoclonal antibody (1:3000, Bio-Rad Laboratories, Hercules, CA, USA), rabbit anti-mouse C-Jun N-terminal kinase (JNK) polyclonal (1:2000, Thermo Scientific Pierce, Rockford, IL, USA), rabbit anti-mouse phosphorylated JNK (p-JNK) polyclonal antibody (1:2000, Sangon Biotech. Co. Ltd., Shanghai, China), rabbit anti-mouse p38 polyclonal antibody (1:3000, Sigma-Aldrich), rabbit anti-mouse p-p38 polyclonal antibody (1:2000, Amresco Inc., Solon, OH, USA) and rabbit anti-mouse glyceraldehyde-3-phosphate dehydrogenase (GAPDH) polyclonal antibody (1:3000, Abcam Biotech., Cambridge, Massachusetts, USA) at room temperature for 2 h. The FVDF membranes were washed with PBST and incubated with horseradish peroxidase (HRP)-conjugated goat anti-rabbit IgG (Abcam Biotech., Cambridge, Massachusetts, USA). Western bands were visualized with the enhanced chemiluminescence (ECL) kit (Thermo Scientific Pierce, Rockford, IL, USA). The western blotting bands were scanned, captured and analyzed with a UVP image scanning system (Mode: GDS8000, Sacramento, CA, USA).

Statistical analysis

All of the data in present study were described as mean ± standard deviation (SD) and analyzed with SPSS software 20.0 (SPSS Inc., Chicago, Ull, USA). The data were obtained from at least three independent experiments. The Student's t test was used for the statistical analysis between two group and One-way ANOVA was used for the statistical analysis of multiple groups. A statistical significance was defined when $P<0.05$.

Results

MRI exhibited the lesion site of EAE animal models

In order to identify the lesion site of the EAE animal models, the MRI inspection was con-

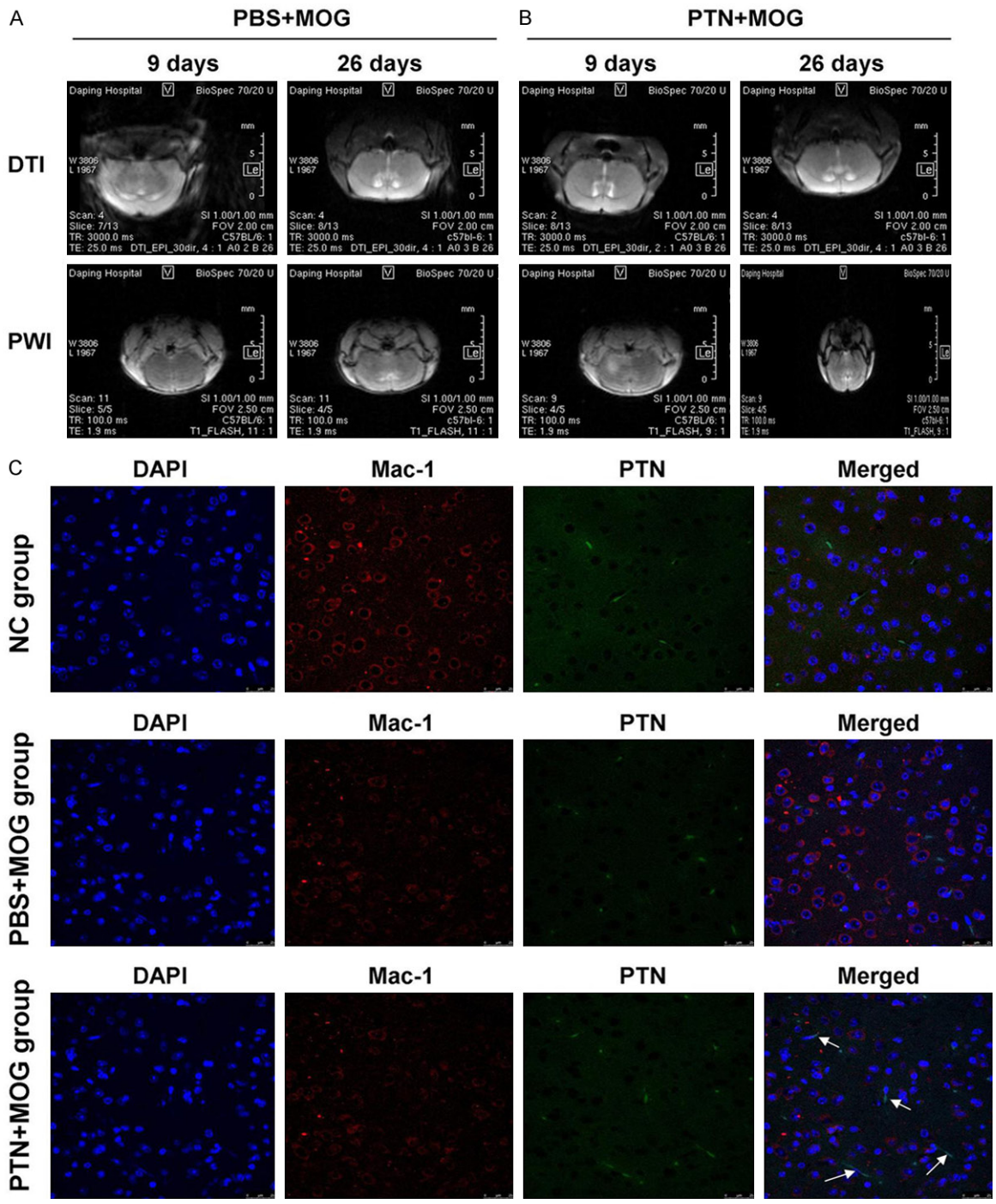

Figure 2. Imaging for DTI and PWI of EAE animal models and co-localization evaluation of Mac-1 and PTN in microglia cells. A. The DTI and PWI images in PBS+MOG group at 9 and 26 days. B. The DTI and PWI images in PTN+MOG group at 9 and 26 days. C. Co-localization of Mac-1 and PTN in microglia cells examined using immunofluorescence double label assay. White arrows represent the co-localized Mac-1 and PTN (Merged staining cells).

ducted in this study. The diffusion tensor imaging (DTI) and perfusion imaging (PWI) images were captured at day 9 post the immunization and day 26 post the immunization, respectively. Both of the DTI and PWI images in PBS+MOG (**Figure 2A**) and PTN+MOG group (**Figure 2B**) showed that the lesion sites mainly appeared in NAWM of bilateral occipital lobes. Therefore, in the following experiments, we focused on the NAWM as lesion site in of EAE animal model.

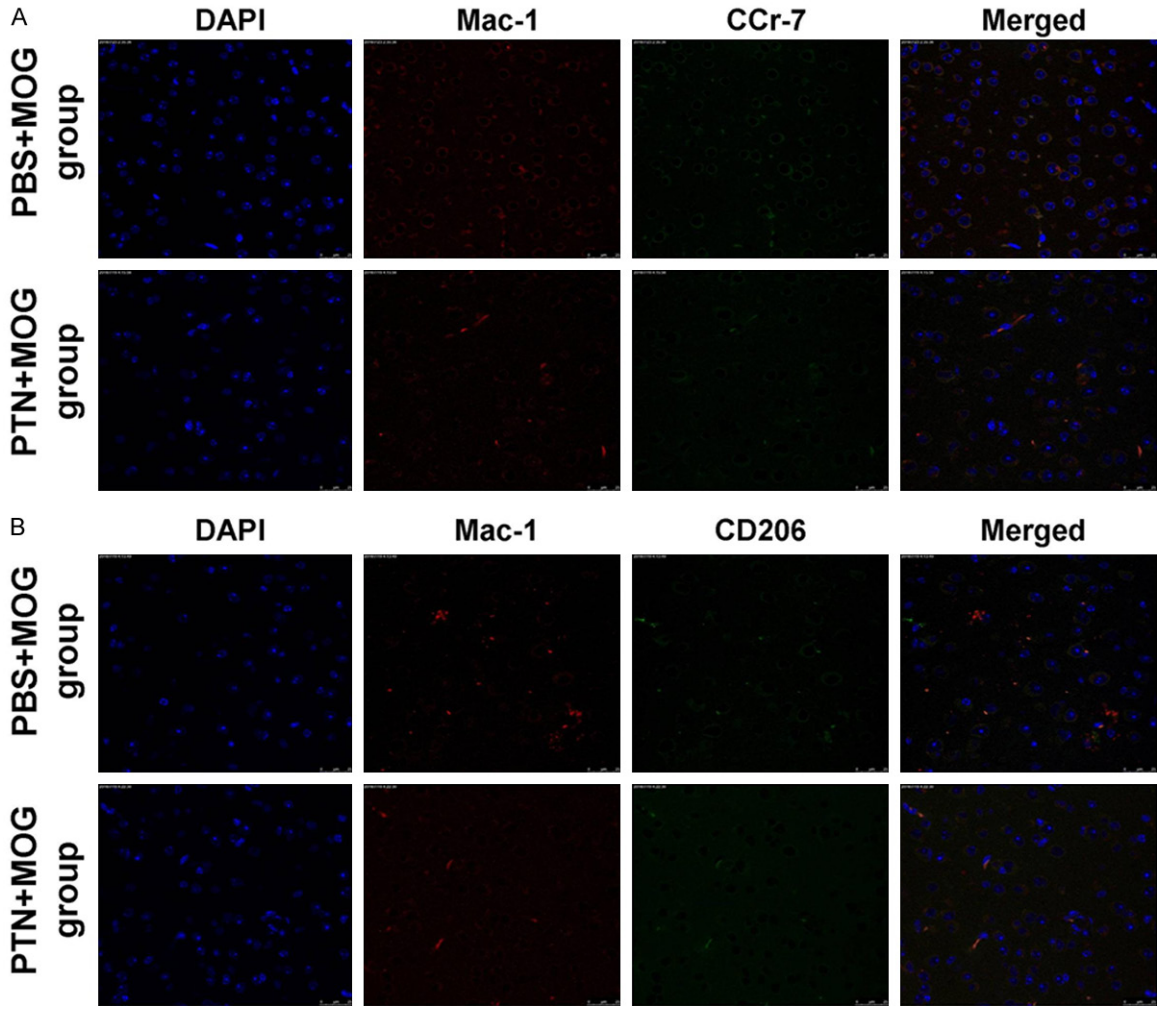

Figure 3. Co-localization of Mac-1 and CCr-7 or CD206 in microglia cells examined using immunofluorescence double label assay. A. Co-localization of Mac-1 and CCr-7 in microglia cells. B. Co-localization of Mac-1 and CD206 in microglia cells.

PTN mainly expressed in microglia cells of EAE models

Immunofluorescence double label assay was performed to examine expression of PTN in EAE models. In this study we selected the Mac-1 molecule as biomarker for microglia cells [25]. Therefore, the results showed that the PTN and Mac-1 co-localized in microglia cells, which suggested that PTN was expressed in microglia cells. Therefore, the results indicated that there were more PTN stained microglia cells in PTN+MOG group compared to both NC group and PBS+MOG group (**Figure 2C**).

PTN treatment enhanced CCr7 and reduced CD206 expression

In order to observe the evolution process of functional heterogeneity of microglia cells, the immunofluorescence double label assay was conducted. The results showed that the positively merged staining microglia cells were significantly enhanced in PTN+MOG group compared to that of PBS+MOG group (**Figure 3A**). However, the positively merged staining microglia cells in PTN+MOG group were significantly reduced compared to that of PBS+MOG group (**Figure 3B**).

PTN participated in mitogen-activated protein kinase (MAPK) signaling pathway in EAE models

The MAPK signaling pathway key biomarkers [26], including ERK1/2, JNK and p38, were examined by using immunofluorescence double label assay. The results showed that levels of p-ERK1/2 in microglia cells of EAE models

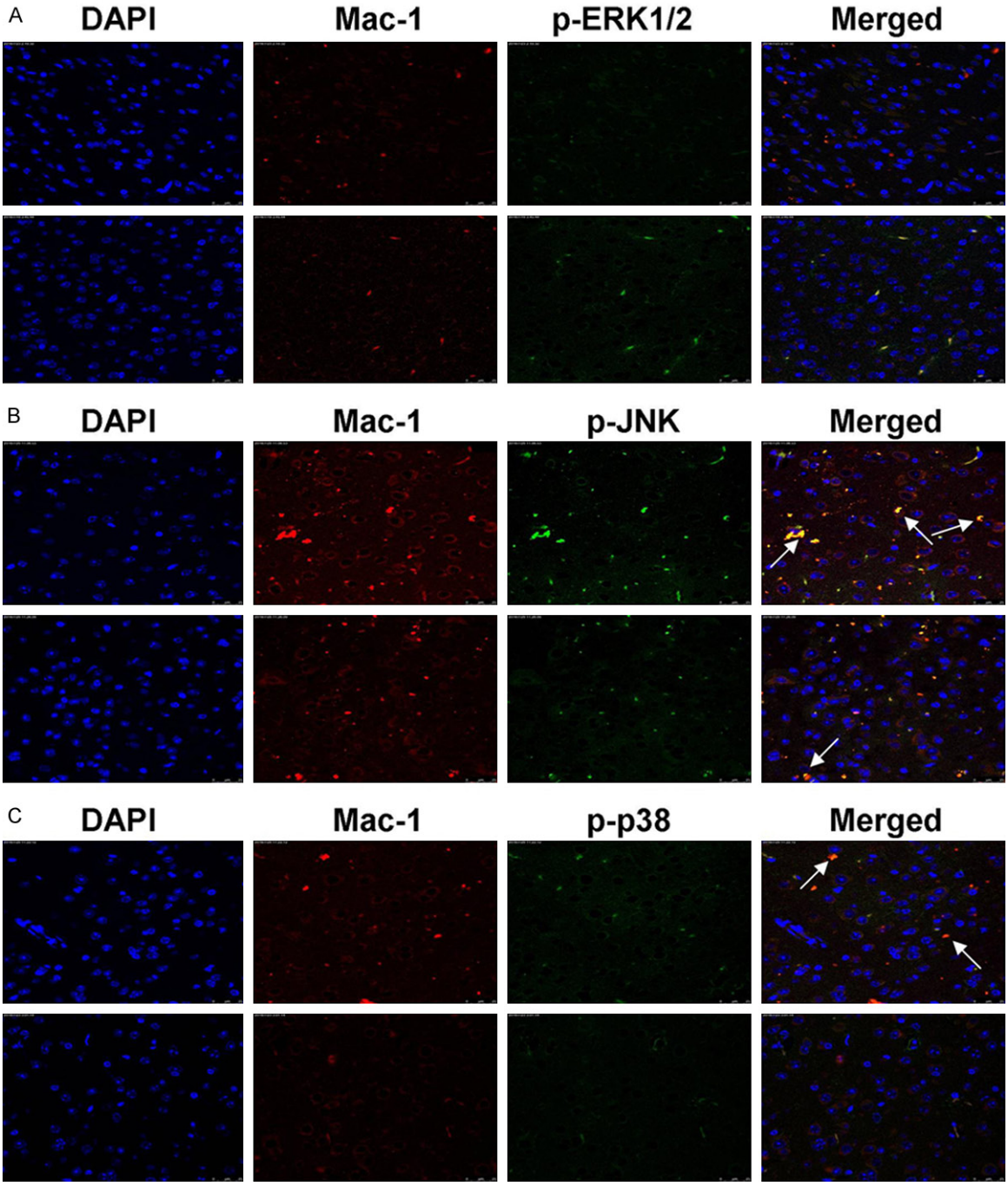

Figure 4. Co-localization of Mac-1 and p-ERK1/1, p-JNK, p-p38 in microglia cells examined using immunofluorescence double label assay. A. Co-localization of Mac-1 and p-ERK1/2 in microglia cells. B. Co-localization of Mac-1 and p-JNK in microglia cells. C. Co-localization of Mac-1 and p-p38 in microglia cells. White arrows represent the co-localized Mac-1 and p-ERK1/1, p-JNK or p-p38 (Merged staining cells).

were significantly increased in PTN+MOG group compared to that in PBS+MOG group (**Figure 4A**, $P<0.05$). However, the levels of p-JNK (**Figure 4B**) and p-p38 (**Figure 4C**) in microglia cells of EAE models were significantly decreased in PTN+MOG group compared to that of PBS+MOG group ($P<0.05$).

PTN treatment regulated functional cytokines in M1 and M2 type microglia cells

In this study, the functional cytokines secreted by M1 type microglia cells, such as TNF-α and IL-18, and functional cytokines secreted by M2 type microglia cells, such as IL-10 and TGF-β,

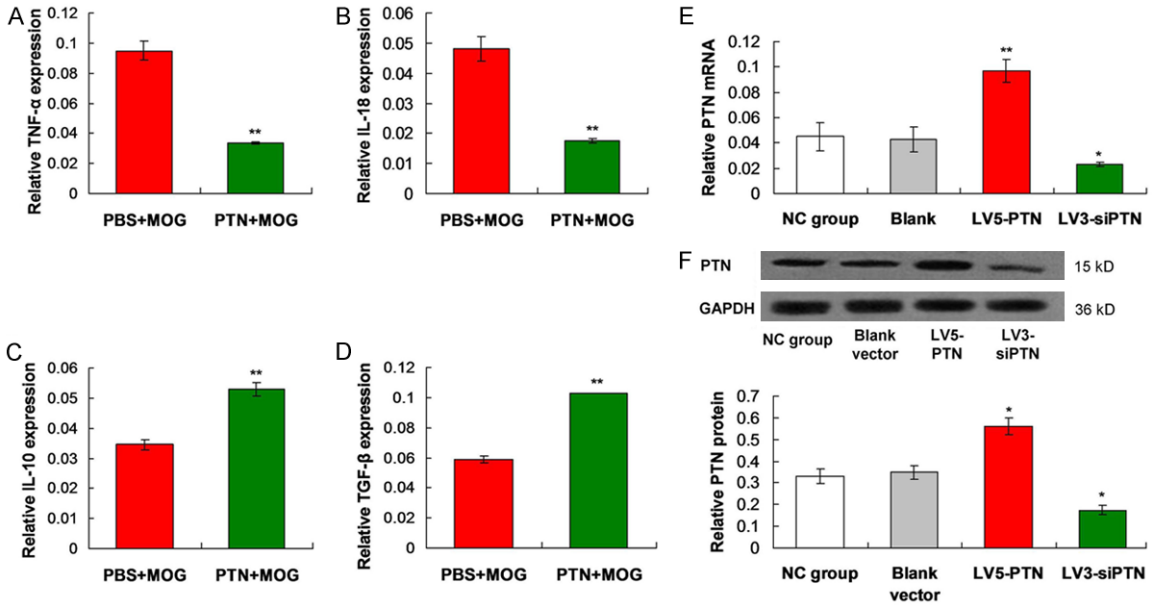

Figure 5. Examination for functional cytokines expression in both M1 type and M2 type microglia cells and determination for PTN expression in LV5-PTN and LV3-siPTN transfected microglia cells. A. Statistical analysis for the TNF-α expression detecting by RT-PCR assay in M1 type microglia cells. B. Statistical analysis for the IL-18 expression detecting by RT-PCR assay in M2 microglia cells. C. Statistical analysis for the IL-10 expression detecting by RT-PCR assay in M2 type microglia cells. D. Statistical analysis for the TGF-β expression detecting by RT-PCR assay in M2 type microglia cells. $**P<0.01$ *vs.* PBS+MOG group. E. mRNA levels of PTN in LV5-PTN and LV3-siPTN transfected microglia cells. F. PTN protein expressions in LV5-PTN and LV3-siPTN transfected microglia cells. $*P<0.05$, $**P<0.01$ *vs.* NC group.

were examined [27]. The results showed that the levels of TNF-α (**Figure 5A**) and IL-18 (**Figure 5B**) secreted by M1 type microglia cells were significantly decreased in PTN+MOG group compared to that of PBS+MOG group ($P<0.05$). Meanwhile, the levels of IL-10 (**Figure 5C**) and TGF-β (**Figure 5D**) secreted by M2 type microglia cells were significantly increased in PTN+MOG group compared to that of PBS+MOG group ($P<0.05$).

LV5-PTN and LV3-siPTN transfection modulated levels of PTN in microglia cells

In order to verify the efficacy of transfection, the PTN expression in LV5-PTN and LV3-siPTN groups was evaluated by using qRT-PCR and western blot assay, respectively. The results indicated that both of the PTN mRNA (**Figure 5E**) and protein (**Figure 5F**) levels were significantly increased in LV5-PTN group and significantly decreased in LV3-siPTN group compared to that of NC or Blank group ($P<0.05$).

PTN modulated MAPK molecules in microglia cells undergoing M1 or M2 inducer treatment

The microglia cells in NC group, Blank vector group, LV5-PTN group and LV3-siPTN group were treated with M1 inducer and M2 inducer, respectively. In this study, the MAPK molecules in above groups were examined by using western blot assay (**Figure 6A**). The results indicated that the PTN significantly modulated the p-ERK5 (**Figure 6B**), p-ERK1/2 (**Figure 6C**), p-p38 (**Figure 6D**) and p-JNK (**Figure 6E**) expression of microglia cells undergoing M1 or M2 inducer treatment, in both LV5-PTN group and LV3-siPTN group compared to that of NC group or Blank vector group (all $P<0.05$). However, there were no effects of PTN treatment on expression of ERK5, ERK1/2, p38 and JNK molecules of microglia cells undergoing M1 or M2 inducer treatment.

PTN promoted the microglia cell transformation from M1 to M2

The results illustrated that the CCr7 levels in LV5-PTN+M1 inducer group were significantly decreased compared to the Blank+M1 inhibitor group (**Figure 7A**, $P<0.05$). Meanwhile, the CD206 levels in LV5-PTN+M2 inducer group were significantly increased compared to that of the Blank+M2 inhibitor group (**Figure 7B**, $P<0.05$). Moreover, the LV3-siPTN acted the adverse effects compared to that of the LV5-

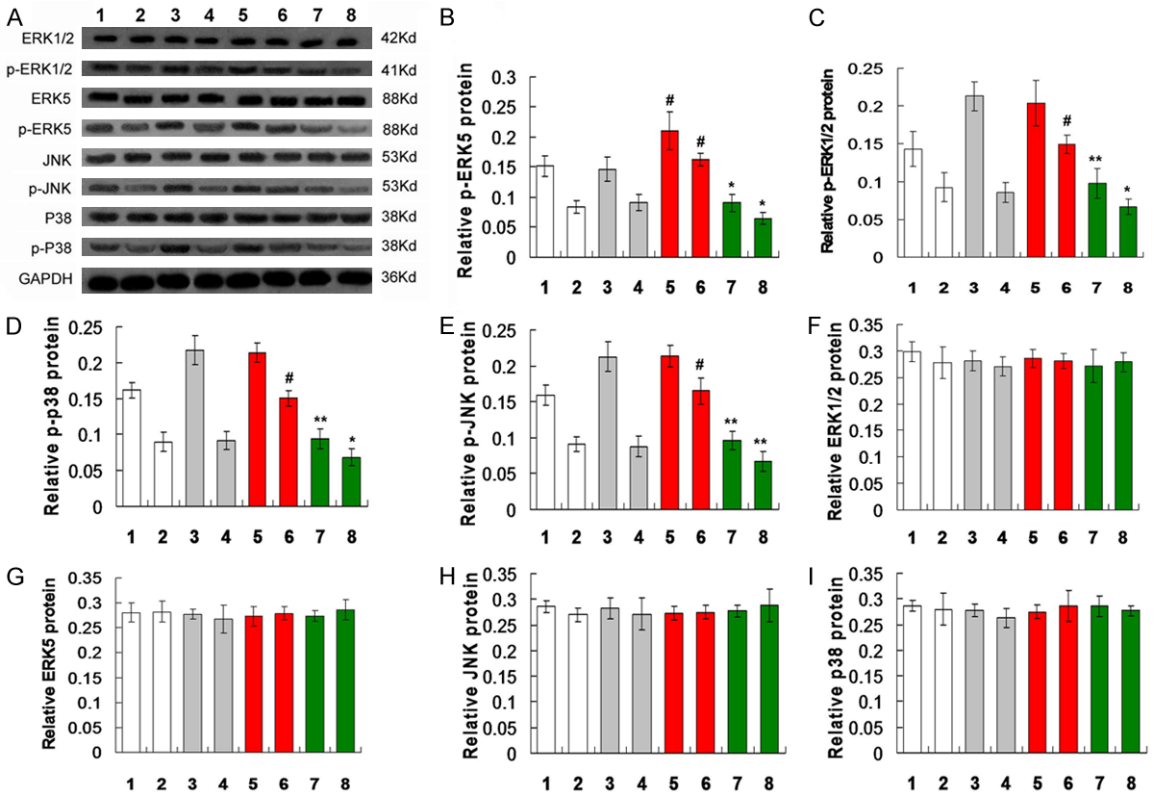

Figure 6. Evaluation for the MAPK molecules expression in microglia cells undergoing M1 or M2 inducer treatment. A. Western blot assay for MAPK molecules expression. B. Statistical analysis for p-ERK5 expression. C. Statistical analysis for p-ERK1/2 expression. D. Statistical analysis for p-p38 expression. E. Statistical analysis for p-JNK expression. F. Statistical analysis for ERK1/2 expression. G. Statistical analysis for ERK5 expression. H. Statistical analysis for JNK expression. I. Statistical analysis for p-p38 expression. 1. NC+M1 inducer, 2. NC+M2 inducer, 3. Blank vector+M1 inducer, 4. Blank vector+M2 inducer, 5. LV5-PTN+M1 inducer, 6. LV5-PTN+M2 inducer, 7. LV3-siPTN+M1 inducer, 8. LV3-siPTN+M2 inducer. *P<0.05, **P<0.01, #P<0.05 *VS.* NC+M1 INDUCER OR NC+M2 inducer group.

PTN treatment for the transformation (**Figure 7**).

PTN strengthened the M1/M2 transformation by regulating functional cytokines

In order to further confirm the PTN induced M1/M2 transformation, the functional cytokines were examined in all of the M1 or M2 inducer treated microglia cells. The results indicated that the levels of M1 microglia cells secreted functional cytokines, TNF-α (**Figure 8A**) and IL-18 (**Figure 8B**), in LV3-siPTN group were significantly increased compared to that of Blank group (P<0.05). Furthermore, the levels of M2 microglia cells secreted functional cytokines, IL-10 and TGF-β, in LV5-PTN group were significantly increased compared to that of Blank group (P<0.05).

Discussion

Nowadays, to reduce or inhibit rates of MS progression, a large numbers of immuno-suppressive and immuno-modulatory agents or drugs have been extensively discovered and applied in clinical [28]. PTN is a kind of cytokine, the expression of which is highly up-regulated in the diverse-pathologies for central nervous system [29]. The diverse-pathologies of central nervous system mainly characterizes by the overt-neuro-inflammation, including ischemia, addictive diseases, neurodegenerative disorders, neuropathic pain [30, 31]. PTN mainly expresses and distributes in the brain during the embryonic development and always be up-regulated in the damaged neurons or neural tumors, such as glioma [32]. Therefore, we investigated the effects of PTN on the functional heterogeneity of microglia cells in MS animal models.

In this study, we firstly established the EAE mouse models of multiple sclerosis. EAE model is a kind of adequate model for remitting and relapsing MS. MS model mainly characterizes by the remission periods and relapse period of

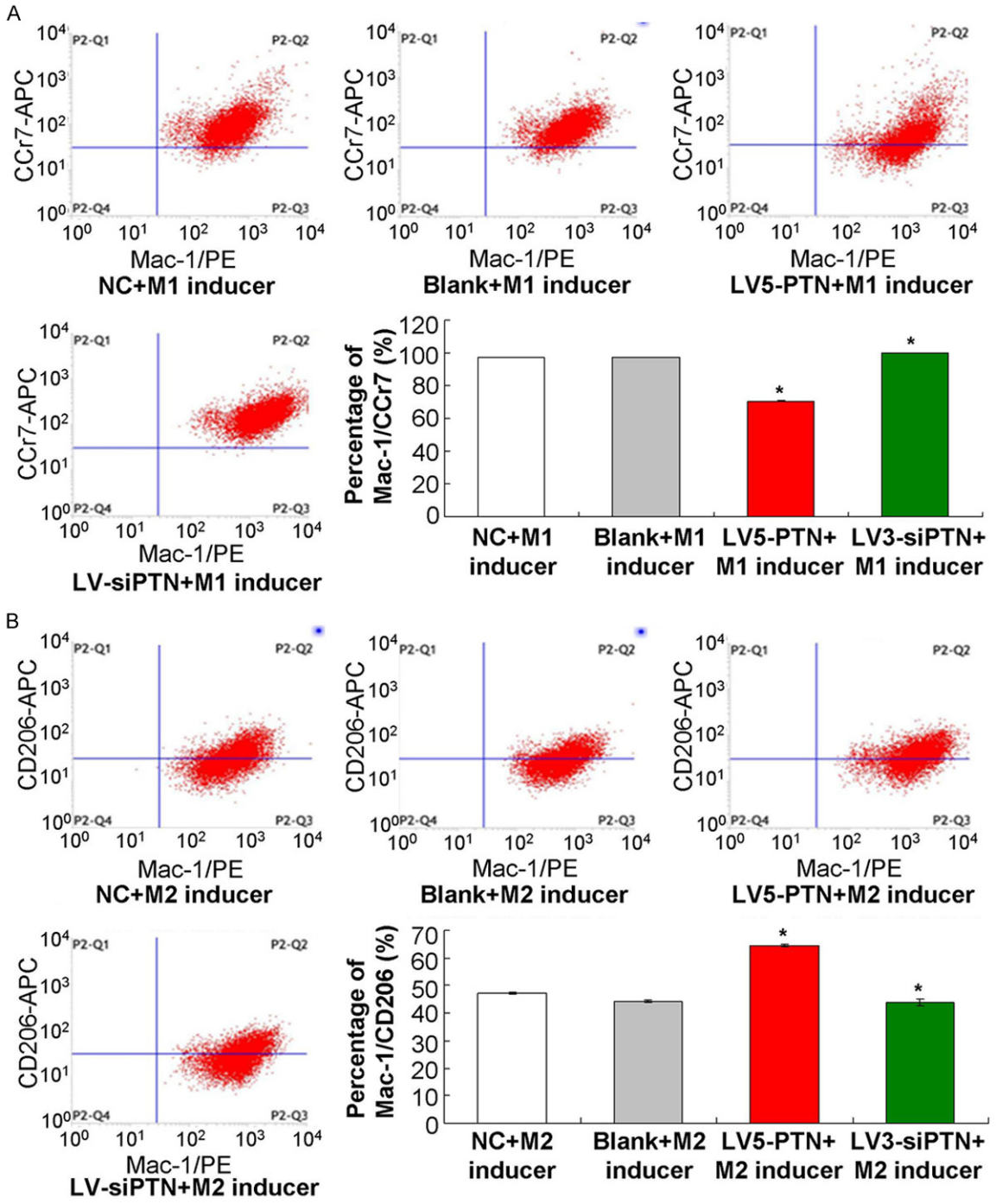

Figure 7. CCr7 and CD206 distribution in microglia cells undergoing M1 or M2 inducer treatment. A. CCr7 expression in microglia cells. B. CD206 expression in microglia cells. **P<0.05, **P*<0.01 vs. NC+M1 inducer or NC+M2 inducer group.

clinical symptoms responding to the infiltrating inflammatory cells [11]. The MRI technology is extensively used in the injury lesions inspection in MS patients or animal EAE model [33]. In our study, the DTI images showed that the lesion sites of MS mainly distributed in the NAWM of bilateral occipital lobes. Therefore, we mainly focused on the NAWM regions as the lesion site in of EAE animal model in the following experiments. Meanwhile, the immunofluorescence double label assay was also conducted to examine the PTN levels of NAWM in the PTN

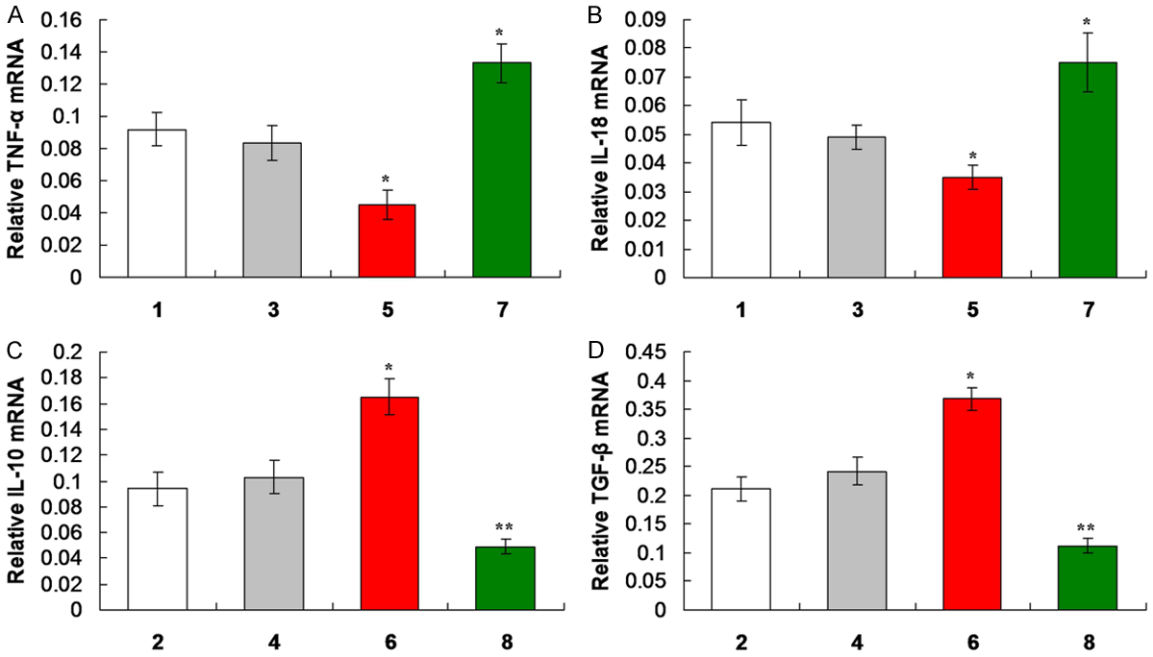

Figure 8. Evaluation for functional cytokines expression in microglia cells undergoing M1 inducer or M2 inducer treatment. A. Statistical analysis for the TNF-α expression in microglia cells undergoing M1 inducer treatment. B. Statistical analysis for the IL-18 expression in microglia cells undergoing M1 inducer treatment. C. Statistical analysis for the IL-10 expression in microglia cells undergoing M2 inducer treatment. D. Statistical analysis for the TGF-β expression in microglia cells undergoing M2 inducer treatment. *P<0.05, **P<0.01 *vs.* NC+M1 inducer or NC+M2 inducer group.

treated EAE models. The Mac-1 molecule is the key biomarker for the microglia cells, therefore, we conducted the immunofluorescence double label assay for co-localizing the PTN and Mac-1 and confirm the expression of PTN in EAE models. The results showed that the TPN expression was significantly increased in PTN+MOG group compared to that of PBS+MOG group, which suggests that PTN also targeted the NAWM regions and is consistent with previous study [34]. Meanwhile, the results also hint that the NAWM could be selected as a candidate of therapeutic size by the PTN in MS therapy.

The biomarkers of functional heterogeneity of microglia cells, CCr7 (for M1 type microglia cells) and CD206 (for M2 type microglia cells) [35], have also been analyzed by using the immunofluorescence double label assay. Our results indicated that the CCr-7 and CD206 positive stained microglia cells were obviously enhanced in PTN+MOG group compared to that of PBS+MOG group for the *in vivo* experiment. Meanwhile, CCr7 levels in LV5-PTN+M1 inducer group were significantly decreased compared to that of Blank+M1 inhibitor group, which suggests that PTN promoted the transformation from M2 to M1 microglia cells. The CD206 levels in LV5-PTN+M2 inducer group were significantly increased compared to that of Blank+M2 inhibitor group, which suggests that PTN promoted the transformation from M1 to M2 microglia cells. Moreover, the LV3-siPTN acted the adverse effects compared to that of LV5-PTN treatment for the transformation. The above data showed that the CCr-7 and CD206 changed following with the treatment of the PTN in both *in vivo* and *in vitro* experiments. All of the CCr-7 and CD206 findings suggest that PTN participated in modulation of functional heterogeneity of microglia cells.

The *in vivo* experiments showed that levels of p-ERK1/2 were significantly increased, p-JNK and p-p38 levels were significantly decreased in microglia cells of EAE models in PTN+MOG group compared to that in PBS+MOG group. This result suggests that the PTN participated in mitogen-activated protein kinase (MAPK) signaling pathway [26, 36] in EAE models. Moreover, the *in vitro* experiments also showed that the PTN significantly modulated the

p-ERK5, p-ERK1/2, p-p38 and p-JNK expression of microglia cells undergoing M1 or M2 inducer treatment, in both LV5-PTN group and LV3-siPTN group compared to that of NC group or Blank vector group. These results suggest that the PTN modulated MAPK molecules in microglia cells undergoing M1 or M2 inducer treatment *in vitro* levels. However, the levels of p-ERK1/2 *in vivo* experiments were decreased, and the levels of p-ERK1/2 *in vitro* were increased, it seems controversial. Actually, for the molecules of MAPK signaling pathway, there are many factors affecting the changes or expression of the protein kinases, such as the p-ERK1/2. In the following study, we would clarify the mechanisms for the changes of p-ERK1/2 in both *in vivo* and *in vitro* levels.

Furthermore, the levels of the regulating functional cytokines of M1/M2 transformation [37] were also evaluated in M1 or M2 inducer treated microglia cells. Actually, the regulating functional cytokines of M1 type microglia cells include TNF-α and IL-18, and regulating functional cytokines of M2 type microglia cells include IL-10 and TGF-β [27]. Our results showed that levels of TNF-α and IL-18 secreted by M1 type microglia cells were significantly decreased in PTN+MOG group compared to that of PBS+MOG group. Meanwhile, levels of IL-10 and TGF-β secreted by M2 type microglia cells were significantly increased in PTN+MOG group compared to that of PBS+MOG group. The present results also indicated that levels of M1 microglia cells secreted TNF-α and IL-18 in LV3-siPTN group were significantly increased compared to that of Blank group, which suggests that PTN could regulate the transformation of microglia cells from M2 to M1 type. Furthermore, levels of M2 microglia cells secreted IL-10 and TGF-β in LV5-PTN group were significantly increased compared to that of Blank group, which suggests that the PTN could also regulate the transformation of microglia cells from M1 to M2 type. Totally, the present study suggests that PTN plays important roles for triggering the microglia cells from the M2 type to M1 as well as from the M1 type to M2 type. The conclusion of this study is critical for the future investigation for discovering drugs targeting the pathogenesis of MS in clinical.

In conclusion, the lesion sites mainly appeared in the NAWM of bilateral occipital lobes. PTN mainly expressed in microglia cells of EAE models, and enhanced CCr7, reduced CD206 expression both *in vivo* and *in vitro* levels. PTN participated in mitogen-activated protein kinase (MAPK) signaling pathway in EAE models and regulated functional cytokines in both M1 and M2 type microglia cells treated with or without M1 or M2 inducer. PTN promoted the M1/M2 transformation by regulating the CCr-7/CD206 molecules and functional cytokines. Totally, PTN regulated functional heterogeneity of microglia cells of EAE animal models of MS by activating CCr-7/CD206 molecules and functional cytokines. PTN could be considered as a promising candidate molecule for treating early injuries of white matter of MS patients.

Acknowledgements

This study was funded by funds from National Natural Science Foundation(No. 81400984), Natural Science Foundation of Fujian Province (No. 2014D009), the National Health and Family Planning Commision' Scientific Research Foundation-Health and Education cooperation foundation (WKJ2016-2-17) and Fujian Province Health project of innovative medical talents training and Medical innovation project (2017-CXB-22).

Disclosure of conflict of interest

None.

Address correspondence to: Dr. Cina Zheng, Magnetic Resonance Center, Zhongshan Hospital, Xiamen University, 201 Hubinnan Road, Xiamen 361004, China. E-mail: mycinema1@outlook.com; Dr. Guohong Zhuang, Organ Transplantation Institute, Anti-Cancer Research Center, Medical College, Xiamen University, Xiamen 361000, China. E-mail: zghxmu@163.com

References

[1] de Paula Faria D, Vlaming ML, Copray SC, Tielen F, Anthonijsz HJ, Sijbesma JW, Buchpiguel CA, Dierckx RA, van der Hoorn JW, de Vries EF. PET imaging of disease progression and treatment effects in the experimental autoimmune encephalomyelitis rat model. J Nucl Med 2014; 55: 1330-1335.

[2] Qi Q, Mao Y, Tian Y, Zhu K, Cha X, Wu M, Zhou X. Geniposide inhibited endothelial-mesenchymal transition via the mTOR signaling pathway in a bleomycin-induced scleroderma mouse model. Am J Transl Res 2017; 9: 1025-1036.

[3] Mayr WT, Pittock SJ, McClelland RL, Jorgensen NW, Nosewrothy JH, Rodriguez M. Incidence and prevalence of multiple sclerosis in olmsted country minnesota, 1985-2000. Neurology 2003; 61: 1373-1377.
[4] Klaren RE, Motl RW, Woods JA, Miller SD. Effects of exercise in experimental autoimmune encephalomyelitis (an animal model of multiple sclerosis). J Neuroimmunol 2014; 274: 14-19.
[5] Noyes K, Weinstock-Guttman B. Impact of diagnosis and early treatment on the course of multiple sclerosis. Am J Manag Care 2013; 19: S321-S331.
[6] Yadav SK, Mindur JE, Ito K, Dhib-Jalbut S. Advances in the immunopathogenesis of multiple sclerosis. Curr Opin Neurol 2015; 28: 206-219.
[7] Thone J, Ellrichmann G. Oral available agents in the treatment of relapsing remitting multiple sclerosis: an overview of merits and culprits. Drug Health Patient Saf 2015; 5: 37-47.
[8] Goodin DS. Glucocorticoid treatment of multiple sclerosis. Handb Clin Neurol 2014; 122: 455-464.
[9] Donia M, Mangano K, Quattrocchi C. Specific and strain-independent effects of dexamethasone in the prevention and treatment of experimental autoimmune encephalomyelitis in rodents. Scand J Immunol 2010; 72: 396-407.
[10] Jonkman LE, Soriano AL, Amor S, Barkhof F, van der Valk P, Vrenken H, Geurts JJ. Can MS lesion stages be distinguished with MRI? A postmortem MRI and histopathology study. J Neurol 2015; 262: 1074-1080.
[11] van Noort JM, Bsibsi M, Gerritsen WH, van der Valk P, Bajramovic JJ, Steinman L, Amor S. Alphab-crystallin is a target for adaptive immune responses and a trigger of innate responses in preactive multiple sclerosis lesions. J Neuropathol Exp Neurol 2010; 69: 694-703.
[12] van Horssen J, Singh S, van der Pol S, Kipp M, Lim JL, Peferoen L, Gerritsen W, Kooi EJ, Witte ME, Geurts JJ. Clusters of activated microglia in normal-appearing white matter show signs of innate immune activation. J Neuroinflammation 2012; 9: 156.
[13] Liu C, Li Y, Yu J, Feng L, Hou S, Liu Y, Guo M, Xie Y, Meng J, Zhang H. Targeting the shift from M1 to M2 macrophages in experimental autoimmune encephalomyelitis mice treated with fasudil. PLoS One 2013; 8: e54841.
[14] Jiang Z, Jiang JX, Zhang GX. Macrophages: a double-edged sword in experimental autoimmune encephalomyelitis. Immunol Lett 2014; 160: 17-22.
[15] Zhang Z, Zhang ZY, Schittenhelm J, Wu Y, Meyermann R, Schluesener HJ. Parenchymal accumulation of CD163+ macrophages/microglia in multiple sclerosis brains. J Neuroimmunol 2011; 237: 73-79.
[16] Zeis T, Graumann U, Reynolds R, Schaeren-Wiemers N. Normal-appearing white matter in multiple sclerosis is in a subtle balance between inflammation and neuroprotection. Brain 2008; 131: 288-303.
[17] Paveliev M, Fenrich KK, Kislin M, Kuja-Panula J, Kulesskiy E, Varjosalo M, Kajander T, Mugantseva E, Ahonen-Bishopp A, Khiroug L, Kulesskaya N, Rougon G, Rauvala H. HB-GAM (pleiotrophin) reverses inhibition of neural regeneration by the CNS extracellular matrix. Sci Rep 2016; 6: 33916.
[18] Kuboyama K, Fujikawa A, Suzuki R, Noda M. Inactivation of protein tyrosine phosphatase receptor type z by pleiotrophin promotes remyelination through activation of differentiation of oligodendrocyte precursor cells. J Neurosci 2015; 35: 12162-12171.
[19] Yeh HJ, He YY, Xu J, Hsu CY, Deuel TF. Upregulation of pleiotrophin gene expression in developing microvasculature, macrophages, and astrocytes after acute ischemic brain injury. J Neurosci 1998; 18: 3699-3707.
[20] Miao J, Ding M, Zhang A, Xiao Z, Qi W, Luo N, Di W, Tao Y, Fang Y. Pleiotrophin promotes microglia proliferation and secretion of neurotrophic factors by activating extracellular signal-regulated kinase 1/2 pathway. Neurosci Res 2012; 74: 269-276.
[21] Kim KY, Scholl ES, Liu X, Shepherd A, Haeseleer F, Lee A. Localization and expression of CaBP1/caldendrin in the mouse brain. Neuroscience 2014; 268: 33-47.
[22] Wang L, Zhai W, Yang X, Wang F, Li J, Li Q, Li Y. Lentivirus-mediated stable Fas gene silencing in human umbilical cord-derived mesenchymal stem cells. Nan Fang Yi Ke Da Xue Xue Bao 2014; 34: 1475-1480.
[23] Miller DH, Thompson AJ, Filippi M. Magnetic resonance studies of abnormalities in the normal appearing white matter and grey matter in multiple sclerosis. J Neurol 2003; 250: 1407-1419.
[24] Howell OW, Rundle JL, Garg A, Komada M, Brophy PJ, Reynolds R. Activated microglia mediate axoglial disruption that contributes to axonal injury in multiple sclerosis. J Neuropathol Exp Neurol 2010; 69: 1017-1033.
[25] Wang H, Hong LJ, Huang JY, Jiang Q, Tao RR, Tan C, Lu NN, Wang CK, Ahmed MM, Lu YM, Liu ZR, Shi WX, Lai EY, Wilcox CS, Han F. P2RX7 sensitizes Mac-1/ICAM-1-depedent leukocyte-endothelial adhesion and promotes neurovascular injury during septic encephalopathy. Cell Res 2015; 25: 674-690.
[26] Cheng L, Zhou S, Zhao Y, Sun Y, Xu Z, Yuan B, Chen X. Tanshinone IIA attenuates osteoclasto-

genesis in ovariectomized mice by inactivating NF-kB and akt signaling pathways. Am J Transl Res 2018; 10: 1457-1468.
[27] Tam WY, Ma CH. Bipolar/rod-shaped microglia are proliferating microglia with distinct M1/M2 phenotypes. Sci Rep 2014; 4: 7279.
[28] Soleimani M, Jameie SB, Barati M, Mehdizadeh M, Kerdari M. Effects of coenzyme Q10 on the ratio of TH1/H2 in experimental autoimmune encephalomyelitis model of multiple sclerosis in C57BL/6. Iran Biomed J 2014; 18: 203-211.
[29] Herradon G, Perez-Garcia C. Targeting midkine and pleiotrophin signalling pathways in addiction and neurodegenerative disorders: recent progress and perspectives. Br J Pharmacol 2014; 171: 837-848.
[30] Ezquerra L, Alguacil LF, Nguyen T, Deuel TF, Silos-Santiago I, Herradon G. Different pattern of pleiotrophin and midkine expression in neuropathic pain: correlation between changes in pleiotrophin gene expression and rat strain differences in neuropathic pain. Growth Factors 2008; 26: 44-48.
[31] Gramage E, Herradon G. Connecting parkinson's disease and drug addiction: common players reveal unexpected disease connections and novel therapeutic approaches. Curr Pharm Des 2011; 17: 449-461.
[32] Perez-Pinera P, Berenson JR, Deuel TF. Pleiotrophin, a multifunctional angiogenic factor: mechanisms and pathways in normal and pathological angiogenesis. Curr Opin Hematol 2008; 15: 210-214.
[33] Robinson AP, Harp CT, Noronha A, Miller SD. The experimental autoimmune encephalomyelitis (EAE) model of MS: utility for understanding disease pathophysiology and treatment. Handb Clin Neurol 2014; 122: 173-189.
[34] McClain CR, Sim FJ, Goldman SA. Pleiotrophin suppression of receptor protein tyrosine phosphatase-beta maintains the self-renewal competence of fetal human oligodendrocyte progenitor cells. J Neurosci 2012; 32: 15066-15075.
[35] Barbeck M, Motta A, Migliaresi C, Sader R, Kirkpatrick CJ, Ghanaati S. Heterogeneity of biomarterial-induced multinucleated giant cells: possible importance for the regeneration process? J Biomed Mater Res A 2016; 104: 413-418.
[36] Bowden ET, Stoica GE, Wellstein A. Anti-apoptotic signaling of pleiotrophin through its receptor, anaplastic lymphoma kinase. J Biol Chem 2002; 277: 35862-35868.
[37] Yuan Y, Rangarajan P, Kan EM, Wu Y, Wu C, Ling EA. Scutellarin regulates the Notch pathway and affects the migration and morphological transformation of activated microglia in experimentally induced cerebral ischemia in rats and in activated BV-2 microglia. J Neuroinflammation 2015; 12: 11.